Performance of Cylindrical Plastic Solar Collectors for Air Heating
أداء المجمعات الشمسية البلاستيكية الاسطوانية فى تسخين الهواء

M.K. Bassiouny [a] , A.S. Abdullah [b,*]

[a] *Department of Mech. Power Eng., Faculty of Eng., Menoufia University, Shebin El-Kom, Egypt*
[b] *Department of Mech. Power Eng., Faculty of Eng., Tanta University, Tanta, Egypt*

الخلاصة

تم تقديم دراسة نظرية وعملية تشتمل على تحليل انتقال الحرارة بالحمل والاشعاع المشترك لمسخن هواء شمسى من النوع الاسطوانى المرن ذو مقطع دائرى واخرين ذو مقطع بيضاوى الاول محوره الاكبر ٠,٥٥ م والاخر محوره الاكبر ٠,٦٥ م. يصنع المجمع الشمسي من طبقة بلاستيكية من البولى استيلين ذو الكثافة المنخفضة مع عازل خلفى وتعمل كمصاص أسود وغطاء مكون من طبقتين من البلاستيك الشفاف لنفاذ الاشعة الشمسية ويلتصق الماص والغطاء معا على طول حافتيهما. ينفخ المجمع الشمسى بواسطة الهواء المضغوط المتدفق. تم كتابة برنامج على الحاسب الالى لحساب درجة حرارة الهواء الخارج من المجمع والكفاءة الحرارية له. كذلك تم تعيين رقم نوسلت بين المصاص والهواء المسخن بدلالة رقم رينولدز عمليا. تشير المقارنات بين البيانات العملية والطريقة العددية لكفاءة المجمع الشمسى الى اتفاق جيد. تم ايضا استنباط معادلة تجريبية لرقم نوسلت ومقارنتها مع معادلة تجريبية لمؤلفين اخرين.

Abstract— **A theoretical and experimental study including the combined convective and radiative heat transfer analysis of a flexible cylindrical type solar air – heater for circular and two elliptic shape with 0.55 and 0.65 m major axis are presented. The solar collector is manufactured from LDPE films acting as a black absorber with a back insulation and double transparent covers sealed together along its edges. The collector is to be blown with a flow of pressurized air. A computer program is written for calculating the outlet temperature and collector thermal efficiency. Moreover the Nusselt number between the absorber and the heated air is determined experimentally in relation with the Reynolds number. Comparisons between the experimental data and the theoretical methods for the collector efficiency demonstrate a good agreement. In addition of this, the present experimental results of Nusselt number are correlated and compared with a correlation of another authors.**

Keywords— **solar collectors, air- heaters, theoretical analysis, experimental investigations and performance.**

1. INTRODUCTION

The use of solar energy, especially on a large scale, is very often inhibited by the collectors' cost. Thus, a simpler and less expensive collector could be considered as a contribution to development of this field. Solar energy is the world's most abundant permanent source of energy. The amount of solar energy intercepted by the planet is 170 trillion kW, an amount 5,000 times greater than the sum of all other inputs (terrestrial, nuclear, geothermal, and gravitational energies and lunar gravitational energy). Of this amount 30% is reflected to space, 47% is converted to low- temperature heat and re-radiated to space, 23% powers the evaporation / precipitation cycle of the biosphere, less than ½ % represents the kinetic energy of the wind, waves and in photosynthetic storage in plants.

Solar energy is transmitted from the sun through space to earth by electromagnetic radiation. It must be converted to heat before it can be used in practical heating or cooling systems. Solar energy collectors are the devices used to convert the sun's radiation to heat. They must have surface that efficiently absorbs radiation and converts it to heat, which raised the temperature of the absorbing material. A part of this energy is then removed from the absorbing surface by means of a heat transfer fluid that may be either water or air.

The heating of air using solar energy has been the subject of many articles [1-6]. Flat plate solar collectors are the common services for interception solar heat at low temperatures, and had been used extensively for heating purposes. In the past few years, a considerable number of papers had been published relating to the actual design optimization of parameters and performance of solar-air heaters [7–13]. Most of the work reported in the literature requires a considerable amount of effort for performance prediction of new designs of solar- air heaters. Since the numbers of variables are large, it becomes a tedious job to predict the efficiency of a new heater design.

The performance of a large area plastic solar collector has been the subject of many articles [14 and 15]. Many types of plastic materials were used in order to reduce the investment cost. A

* *corresponding author to provide phone: 0101348879;*
e- mail: asbekhatro@yahoo.com

Accepted November 2, 2011.

mathematical expression for calculating the configuration factor of plastic solar collector was derived and analyzed for part and full-load [16]. The cylindrical plastic solar collector is a practical method for crops dehydration and heating processes. This type of collectors can be manufactured as a cylinder (after blowing) with the upper half of a transparent flexible plastic material and the lower half of a black polyvinyl chloride (PVC). It can be made of different lengths and diameters or aspect ratios with one cover and also with back insulation. The thermal efficiency increases as the collector length increases. This is also due to the increase of the configuration factor with the collector length until reached to 20 m after that no change in configuration factor.

In the present work, a plastic cylinder solar collector is designed. It is made from two types of materials, polyvinyl chloride (PVC) as upper half and lower half is made from low density polyethylene (LDPE). Moreover, the performance of a plastic cylinder solar collector will be studied theoretically and experimentally.

2. PERFORMANCE OF THE SOLAR COLLECTOR

Energy balance of the absorber:

In case of the steady-state conditions, the energy balance of absorber of the solar air- heater, Fig 1, can be formulated by the following relation,

$$\dot{Q}_{S,a} = \dot{Q}_{con,a-f} + \dot{Q}_{r,a-c_2} \qquad (1)$$

Where,

$$\dot{Q}_{S,a} = \alpha_a \tau_{c_2} I_c A_p \qquad (2)$$

$$\dot{Q}_{con,a-f} = h_{con,a-f} A\left(T_a - T_{f,m}\right) \qquad (3)$$

$$\dot{Q}_{r,a-c_2} = \frac{\sigma\ A}{\frac{1}{\varepsilon_a} + \frac{1}{\varepsilon_{c_2}} + \frac{1}{F_{a-c_2}} - 2}\left(T_a^4 - T_{c_2}^4\right) \qquad (4)$$

Inserting eqs.(2-4) into eq.(1), results in

$$\tau_{c_2} I_c \frac{A_p}{A} = h_{cond,a-f} A\left(T_a - T_{f,m}\right) + \frac{\sigma}{\frac{1}{\varepsilon_a} + \frac{1}{\varepsilon_{c_2}} + \frac{1}{F_{a-c_2}} - 2}\left(T_a^4 - T_{c_2}^4\right) \qquad (5)$$

Energy balance of cover :

The energy balance of the cover can be represented, according to Fig.1, by the Following expression .

$$\dot{Q}_{S,c_2} + \dot{Q}_{con,f-c_2} + \dot{Q}_{r,a-c_2} = \dot{Q}_{cond,c_2-c_1} + \dot{Q}_{r,c_2-c_1} \qquad (6)$$

Where,

$$\dot{Q}_{S,c_2} = \alpha_{c_2} * \tau_a * I_c * A_p \qquad (7)$$

$$\dot{Q}_{con,f-c_2} = h_{con,f-c_2} A(T_{f,m} - T_{c_2}) \qquad (8)$$

$$\dot{Q}_{cond,c_2-c_1} = \frac{\pi KL(T_{c_2} - T_{c_1})}{\ln\left(\frac{r_1}{r_2}\right)} \qquad (9)$$

$$\dot{Q}_{r,c_2-c_1} = \frac{\sigma\ A}{\frac{1}{\varepsilon_{c_1}} + \frac{1}{\varepsilon_{c_2}} + \frac{1}{F_{c_2-c_1}} - 2}\left(T_{c_2}^4 - T_{c_1}^4\right) \qquad (10)$$

Substituting eq.(4) and eqs. (7-10) into eq.(6), the following relation yields

$$\alpha_{c_2} * \tau_a * I_c * \frac{A_p}{A} + h_{cond,f-c_2}(T_{f,m} - T_{c_2}) + \frac{\sigma}{\frac{1}{\varepsilon_a} + \frac{1}{\varepsilon_{c_2}} + \frac{1}{F_{a-c_2}} - 2}\left(T_a^4 - T_{c_2}^4\right) =$$

$$\frac{\pi KL(T_{c_2} - T_{c_1})}{\ln\left(\frac{r_1}{r_2}\right)} + \frac{\sigma}{\frac{1}{\varepsilon_{c_1}} + \frac{1}{\varepsilon_{c_2}} + \frac{1}{F_{c_2-c_1}} - 2}\left(T_{c_2}^4 - T_{c_1}^4\right) \qquad (11)$$

Energy balance of cover:

The energy balance of the cover can be represented, according to Fig.1,by the Following expression .

$$\dot{Q}_{S,c_1} + \dot{Q}_{cond,c_2-c_1} + \dot{Q}_{r,c_2-c_1} = \dot{Q}_{con,c_1-\infty} + \dot{Q}_{sky} \qquad (12)$$

Where,

$$\dot{Q}_{S,c_1} = \alpha_{c_1} * I_c * A_p \qquad (13)$$

$$\dot{Q}_{con,c_1-\infty} = h_{con,c_1-\infty} A(T_{c_1} - T_\infty) \qquad (14)$$

$$\dot{Q}_{sky} = A * \varepsilon_{c_1} * \sigma * \left(T_{c_1}^{\ 4} - T_{sky}^{\ 4}\right) \qquad (15)$$

Substituting eqs.(9), (10) and eqs. (13-15) into eq.(12), the following relation yields

$$\alpha_{c_1} * I_c * \frac{A_p}{A} + \frac{\pi KL(T_{c_2} - T_{c_1})}{\ln\left(\frac{r_1}{r_2}\right)} + \frac{\sigma}{\frac{1}{\varepsilon_{c_1}} + \frac{1}{\varepsilon_{c_2}} + \frac{1}{F_{c_2-c_1}} - 2}\left(T_{c_2}^4 - T_{c_1}^4\right) =$$

$$h_{con,c_1-\infty}(T_{c_1} - T_\infty) + \varepsilon_{c_1} * \sigma * \left(T_{c_1}^4 - T_{sky}^4\right) \qquad (16)$$

Energy balance of fluid element:
An energy balance of the fluid element, sketched in Fig.2, gives the following equation:

$$\dot{m}i + q_{con,a-f}\Delta A = \dot{m}(i+\Delta i) + q_{con,f-c_2}\Delta A \quad (17)$$

Substituting eq. (3) into eq. (17) and applying Taylor series gives:

$$\dot{m}i + h_{con,a-f}\left(\frac{1}{2}P\Delta X\right)\left(T_a - T_f(X)\right) = \dot{m}\left(i + \frac{di}{dx}\Delta X\right) + h_{con,f-c_2}\left(\frac{1}{2}P\Delta X\right)\left(T_f(X) - T_{c_2}\right)$$

One obtains, after collecting the terms and putting $i = c_p T_f(X)$,

$$\frac{\dot{m}c_p dT_f(X)}{\frac{1}{2}P\Delta X} = h_{con,a-f}\left(T_a - T_f(X)\right) - h_{con,f-c_2}\left(T_f(X) - T_{c_2}\right)$$

Taking into account that $h_{con,a-f} = h_{con,f-c_2}$,

$$\therefore \frac{\dot{m}c_p dT_f(X)}{\frac{1}{2}P\Delta X} = h_{con,a-f}\left(T_a + T_c - 2T_f(X)\right)$$

Let $NTU = \dfrac{h_{con,a-f}A}{\dot{m}c_p} = \dfrac{h_{con,a-f}\left(\frac{1}{2}PL\right)}{\dot{m}c_p}$

and $x = \dfrac{X}{L}$, we have

$$\frac{dT_f(x)}{dx} = NTU\left(T_a + T_{c_2} - 2T_f(x)\right) \quad (18)$$

The integration of eqn. (18) results in

$$T_f(x) = \frac{1}{2}\left[\left(T_a + T_{c_2}\right) - Ce^{-2NTUx}\right] \quad (19)$$

The boundary conditions associated with eq. (19) are

At x=0, $T_f = T_{in}$ and at x=1, $T_f = T_{out}$

The substitution of the preceding boundary condition in equation (19) gives:

$$T_{out} = \frac{1}{2}\left[\left(T_a + T_{c_2}\right) - \left(T_a + T_{c_2} - 2T_{in}\right)e^{-2NTU}\right] \quad (20)$$

Collector thermal efficiency:
The collector thermal efficiency may be defined and calculated from the following relation.

$$\eta_{th} = \frac{\text{Useful energy delivered}}{\text{total incoming solar energy}} = \frac{\dot{Q}_u}{A_p I_c} = \frac{2\dot{Q}_u}{\pi DLI_c} \quad (21)$$

The useful energy delivered is the energy carried away by the flowing air, which is equal to

$$\dot{Q}_u = \dot{m}c_p\left(T_{out} - T_{in}\right) \quad (22)$$

The substitution of eq. (22) into eq. (21), making use of eq. (20), yields

$$\eta_{th} = \frac{2\dot{m}c_p\left(T_{out} - T_{in}\right)}{\pi DLI_c} = \frac{\dot{m}c_p\left(T_a + T_{c_2} - 2T_{in}\right)\left(1 - e^{-2NTU}\right)}{\pi DLI_c} \quad (23)$$

3. NUMERICAL SOLUTION

Equations (5),(11),(16) and (20) are four simultaneous quartic algebraic equations in the four unknowns cover1, cover2, absorber and air outlet temperatures. These equations can be solved numerically using the *Newton-Raphson* iterative procedure [17]. A computer program was written and developed for solving the above mentioned equations and determining the collector thermal efficiency. The solutions are obtained in terms of the influencing parameters such as the solar insolation, air mass flow rate and air inlet temperature.

4. EXPERIMENTAL INVESTIGATIONS

In order to test the performance of plastic cylindrical-type solar air-heater with different design parameters and under variable operating conditions, an experimental setup is constructed, as shown in Fig.3, in the energy laboratory, Tanta University, Faculty of Engineering. The air-heater, in its simplest design, consists of a plastic hose with 0.50 m diameter and 20 m length. It is made of a black low density polyethylene (LDPE) sheet of 0.7 mm thickness acting as an absorber and two transparent covers of polyvinyl chloride (PVC) sheet having 0.7 mm thickness. The air gap between two covers is made with a thickness of 4cm works as insulation layer. All sheets of absorber and two covers are sealed together along their edges. Holes are made in the edges and ropes are used for the sake of fixation, as represented in Fig.3.
The collector is blown with a flow of pressurized air using an air blower having a maximum discharge of about 1500 m^3/h. The air flow rate is controlled by changing speed of blower. An orifice meter is calibrated with the help of a bellows meter of 0.05 m^3 resolution (for measuring the volume of air) and a stop watch in order to determine the air flow rate

by measuring the pressure drop across it using water U-tube manometer. A Bourdon's tube pressure gauge of 0.1 bar resolution was used for measuring air pressure at tube inlet while a mercury glass thermometer of 0.2 °C resolutions was used for measuring the ambient temperature.

Air temperature measurements are carried out with copper-constantan thermocouple probes of about 1 mm bead diameter. A thermocouple probe located at the center of the inlet section measures the inlet air temperature. The hot air is mixed in a mixing chamber after leaving the solar collector in order to measure the outlet bulk temperature of air using a single thermocouple probe. The covers and absorber temperatures are measured along the solar collector by means of five thermocouple probes clapped on each surface at equal distances. The average temperature of each surface is obtained as the arithmetic mean of the five-thermocouple readings. The readings are observed periodically to check time dependent measurements. After reaching the steady- state condition, all the measured variables are recorded.

Outdoors experimental investigations are carried out under clear skies on three shapes of flexible cylindrical solar air-heaters with double covers and back insulation. A glass wool layer with 7 cm thickness is held on the back side of the absorber to minimize the energy loss through the bottom. In order to compare their performance, the standard test method of the National Bureau of Standards (NBS), Ref. [18], is performed using the instantaneous test procedure.

Nusselt number

The convective heat transfer film coefficient between the absorber and the flowing air can be calculated from the following relation:

$$h_{con,a-f} = \frac{\dot{Q}_u}{A\left(T_a - T_{f,m}\right)} = \frac{\dot{m} c_p \left(T_{out} - T_{in}\right)}{A\left(T_a - T_{f,m}\right)} \qquad (24)$$

Where $T_{f,m}$ is the air mean temperature, which is given by

$$T_{f,m} = \frac{T_{in} - T_{out}}{2} \qquad (25)$$

The Nusselt number is defined as

$$Nu = \frac{h_{con,a-f} D}{k} \qquad (26)$$

5. RESULTS AND DISCUSSION

Figures 4 and 5 indicate the results obtained for collector outlet temperature (T_{out}) through the hours of day. The figures show that the outlet temperature increases gradually with time of day and reach its maximum value at period of 12:00 to 14:00, where maximum solar insolation is occurred. The maximum outlet temperature is attained at the minimum mass flow rate of air (0.13 kg/s), where the low velocities of air make it gains more and more heat energy from the absorber.

Also the figures show that the maximum outlet temperature for the collector with the circular shape is higher than that of the collector with elliptic shape. This is because the collector with circular shape is more concave than elliptic shape. The more concave shape mean high configuration (shape, view) factor and the highest configuration factor led to the highest heat transfer rate from absorber to cover.

The experimental results for the collector outlet temperature against the solar insolation through five days are shown in Fig.6. The average ambient temperature through these days is 31°C. The figure shows that the collector outlet temperature increases linearly with increasing of solar insolation. The increase of solar insolation causes increase in heat gain by absorber which transfers to air passes over the absorber, i.e. increases the collector outlet temperature.

Figures 7, 8 and 9 indicate the experimental results and numerical solution obtained for the collector thermal efficiency against the appropriate parameter $\Delta T/I_c$. The figures show that the collector thermal efficiency decreases linearly with the parameter $\Delta T/I_c$. The former is because the increasing of parameter $\Delta T/I_c$ back to the decreasing of solar insolation (I_c), and due to the decreasing in solar insolation the heat gain by the absorber decreases which leads to decreasing the heat gained by passing air over absorber which decreases the air outlet temperature (T_{out}), where thermal efficiency is a function of ($T_{out} - T_{in}/I_c$), so the thermal

efficiency decreases linearly with the parameter $\Delta T/I_c$.

The comparison between various shapes of collectors is made as shown in Fig. 10. The figure shows that the collector thermal efficiency decreases with increasing the collector major axes. The reason behind that is because the configuration factor between the absorber and the cover becomes lower with increasing the collector major axes. The rate of increase of thermal efficiency is high for circular shape of collector and it becomes relatively insignificant for elliptic shapes.

Inspection of the plotted data in Fig.11 shows that Nu versus Re logarithmic plot is linear. The resulting correlation for Nusselt number between the absorber and the heated air is obtained to be as follows:

$Nu = 0.13 * Re^{0.64}$,

Through comparison of the foregoing developed correlation with the test data, the correlation is found to be fairly representative to the experimental results, as seen from Fig.11. Both the correlation and the test data are compared once more with Dittus- Boelter below equation

$Nu = 0.023\ Re^{0.8}\ Pr^{0.4}$,

with Pr = 0.7 for air and Re is based on the hydraulic diameter. A good agreement is found between the three compared results, as shown in Fig.11.

6. CONCLUSIONS

The performance of a plastic cylindrical solar air-heater with double covers and back insulation is studied theoretically and experimentally, from the standpoint of thermal energy. As a result, the outlet temperature increases gradually with hours of day where the solar insolation increased gradually and reaches its maximum value at 12:00 to 14:00 hrs, during this period the maximum outlet temperature is reached. The maximum outlet temperature is attained at the minimum mass flow rate of air, where the highest value is 80 °C at mass flow rate 0.13 kg/s for circular collector. Also, it is shown that the thermal efficiency decreases linearly with a parameter $\Delta T/I_c$. It also increases with decreasing the major axes of elliptic shape. The rate of increase is high for collector having circular shape. The thermal efficiency of a cylindrical collector having circular shape is higher than that of elliptic shape. So the thermal efficiency increases from 50 % to 62 % at 0.01 of $\Delta T/I_c$. This is because the most concave shape of circular collector absorbs more heat than the concave shape of elliptic collector. A simple correlation for predicting Nusselt number between the absorber and the heated air is developed. The correlation is found to be fairly representative to the experimental data and agrees satisfactorily with a previously published correlation of another author. The included comparisons between the numerical and experimental results show also good agreements.

Nomenclature

Symbol	QUANTITY
A	area, m^2
C	constant
c_p	specific heat at constant pressure, J/kg K
D	diameter of collector, m
h	heat transfer coefficient, W/m^2 K
I_c	solar insolation, W/m^2
I_o	solar constant (I_o = 1353 w /m^2)
i	specific enthalpy, J/kg
k	thermal conductivity of air, W/m.K
L	length of collector, m
m	mass flow rate of air in collector, kg/s
NTU	Number of Transfer Units
P	perimeter, m
p	pressure, pa
Q	rate of heat transfer, W
q	heat flux, W /m^2
r	radius of collector

Greek symbols

α	absorptivity
Δ	difference
ε	emissivity
η	efficiency
ρ	density, kg/m^3
σ	Stefan – Boltzmann constant, (σ = 5.6687 x 10^{-8} W/m^2 k^4)
τ	transmissivity
τ_{atm}	atmospheric transmittance

Subscripts

a	absorber
c	cover

con	convection
f	fluid
in	inlet
m	mean
out	outlet
p	projected
r	radiation
S	solar
th	thermal
u	useful
∞	ambient

RFFRENCES

[1] Suri RK, and Saini JS. performance of single-and Double- Exposure Solar Air-Heaters. Solar Energy, 1969, v 12, p. 525-530.

[2] Malik MA, Buelow FH. "Heat Transfer in a Solar Heated Air Duct-simplified Analysis" in "Heliotechnique and Development" ; 1976, v2, p.31-37, Development Analysis Associates, Cambridge, Massachusetts

[3] Close D. Solar – Air Heaters for Low and Moderate Temperature Applications Solar Energy, 1963, v7, p.117.

[4] Gupta CL, Garg HP. performance studies on solar Air – Heaters. Solar Energy, 1967, v 11, p. 25.

[5] Akpinar E K, and Koçyiğit F. Experimental investigation of thermal performance of solar air heater having different obstacles on absorber plates. International Communications in Heat and Mass Transfer ,April 2010,Volume 37, Issue 4, , P. 416-421

[6] Akpinar E K, and Koçyiğit F. Energy and exergy analysis of a new flat-plate solar air heater having different obstacles on absorber plates. Applied Energy, November 2010,Volume 87, Issue 11, , P. 3438-3450

[7] Soteris A. Kalogirou - Performance of Solar Collectors. Chap. Four, Solar Energy Engineering Processes and Systems, 2009, P. 219-250

[8] Rae SK, Sure RK. Optimization of Flat – plate Solar Collector Area. Solar Energy, 1969, v12, p.531.

[9] Al- Kamala M, Al-Gharries A. Effect of Thermal Radiation In side Solar Air Heaters. Energy Conversion and Management, 1977, v 38, n 14, p. 1451-1458.

[10] Hashemite A. Thermal performance Enhancement by Interaction between the Radiation and Convection in Solar Air Heaters. Renewable Energy, 1997, v 12, n 4, p. 419 – 433.

[11] Ong K. Thermal performance of solar Air Heaters: Mathematical Model and Solution procedure. Solar Energy, 1995, v 55, n 2, p. 93- 109.

[12] Ong K. Thermal performance of solar Air Heaters: Experimental Correlation. Solar Energy, 1995, v55, n 3, pp. 209- 220.

[13] Choudhury C, Chauhan P, Garg H. Desing Curves for Conventional Solar Air Heater. Renewable Energy, 1995, v6, n 7, p. 739-749.

[14] Janjai S., Esper A., Muhlbauer W. Modelling the performance of a large area plastic solar collector. Renewable Energy , 2000, Volume 21, Issues 3-4, 1, P. 363-376

[15] Dorfling C, Hornung CH, Hallmark B, Beaumont RJJ, Fovargue H, Mackley MR. The experimental response and modelling of a solar heat collector fabricated from plastic microcapillary films Solar Energy Materials and Solar Cells, 2010, Volume 94, Issue 7, P. 1207-1221

[16] Bassiouny MK. Numerical and Experimental Studeis on Plastic Solar Air-Heaters for Heating Processes. Mansoura Engineering Jornal (MEJ)-Faculty of Engineering – Mansoura University, Jun 2003,vol. 28, No 2, p. M111-M132.

[17] McCormick JM, Salvadori MG. "Numerical Methods in Fortran" , Fourth Edition, Prentice-Hall, New Delhi, 1985, Chap.4,p.59-68.

[18] Simon FF. Flat plate Solar Collector performance Evaluation with a Solar Simulator as a Basis for Collector Selection and Performance prediction. NASA Rept. TM X-71793, 1975, see also Solar Energy, 1976,v 18 , p.451-466.

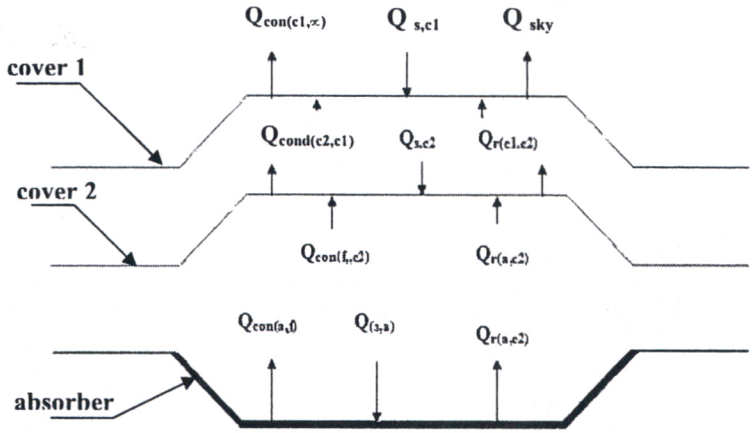

Fig.1 Energy balance of both absorber and covers

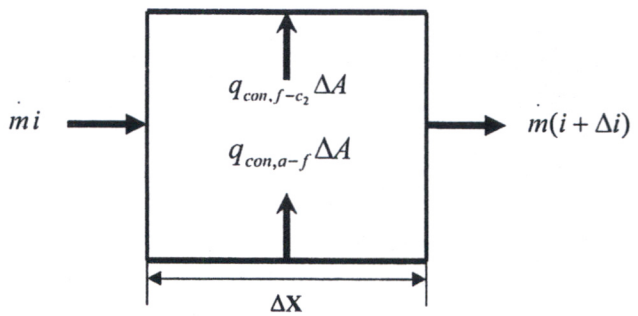

Fig.2: Energy balance of a fluid element

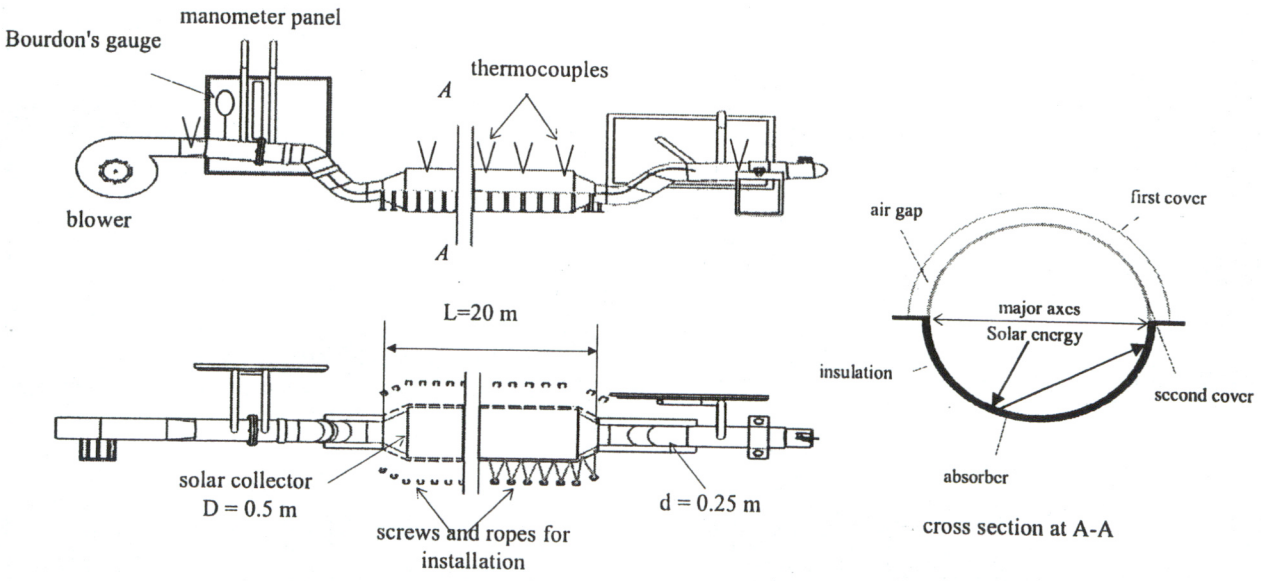

Fig. 3 Experimental setup

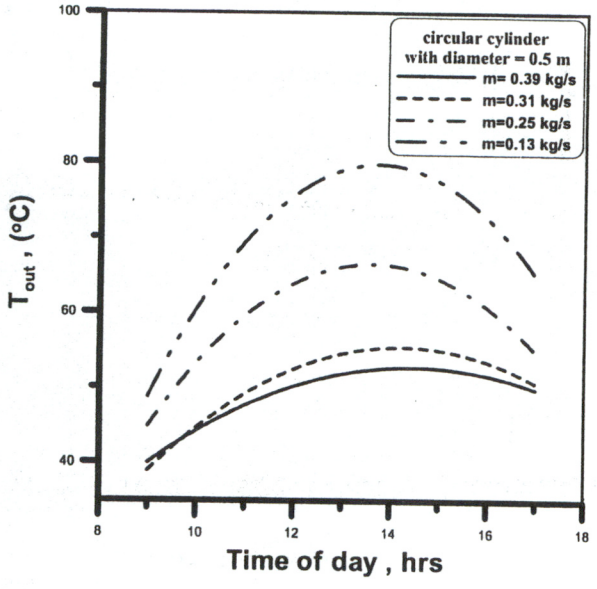

Fig. 4 The outlet temperature through the hours of day for a collector of circular shape with a diameter of 0.50 m.

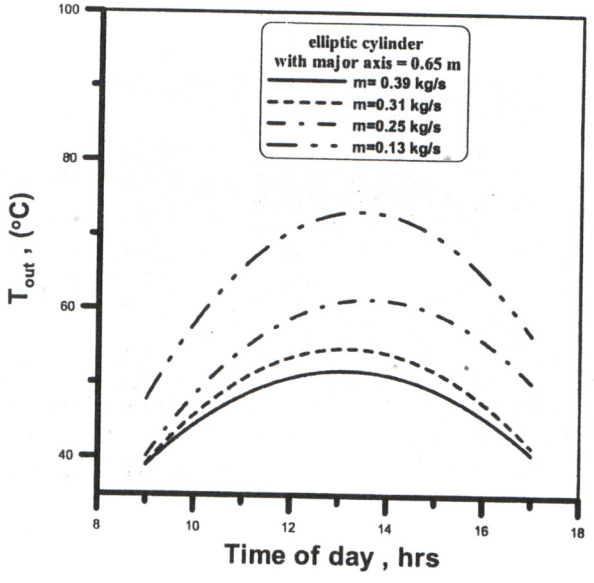

Fig. 5 The outlet temperature through the hours of day for a collector of elliptic shape with a major axis of 0.65 m.

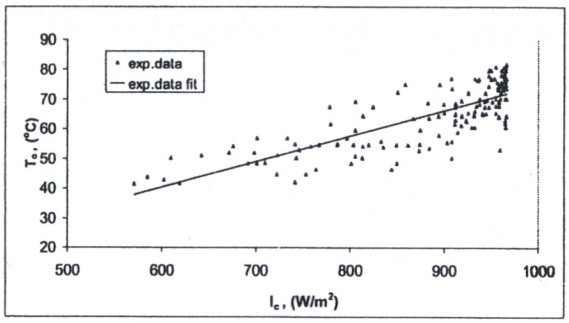

Fig. 6 Experimental collector outlet temperature (T_{out}) against solar insolation (I_c) for a circular collector of diameter 0.50 m.

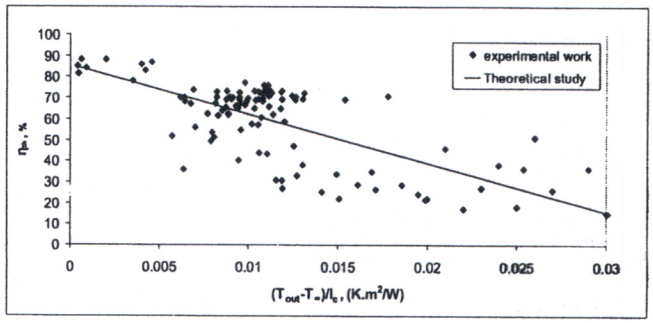

Fig. 7 The experimental results and numerical solution of thermal efficiency against the parameter $\Delta T/I_c$ for a collector of circular shape with diameter 0.50 m.

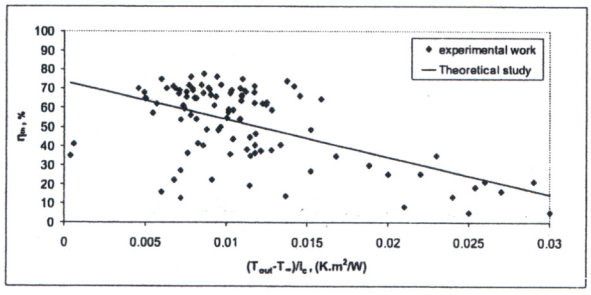

Fig. 8 The experimental and numerical solution of thermal efficiency against the parameter $\Delta T/I_c$ for a collector of elliptic shape with major axis of 0.55 m.

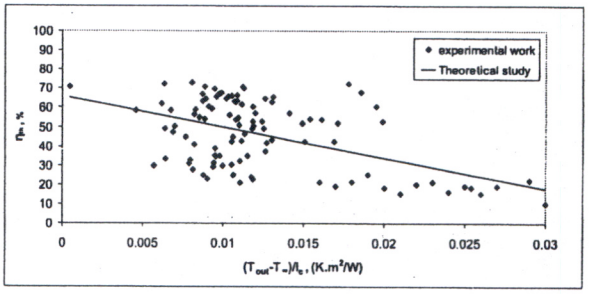

Fig. 9 The experimental and numerical solution of thermal efficiency against the parameter $\Delta T/I_c$ for a collector of elliptic shape with major axis of 0.65 m.

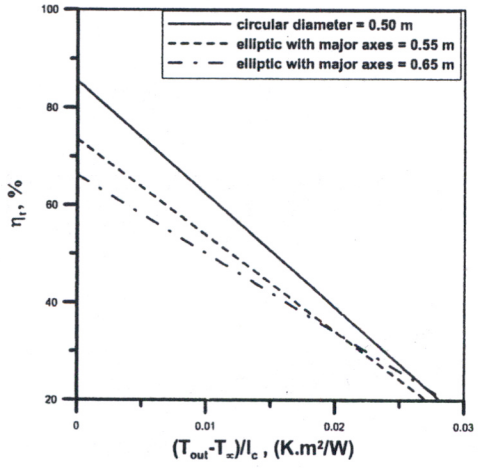

Fig .10 Comparison of the thermal efficiency for the three shapes of solar air-heater collector.

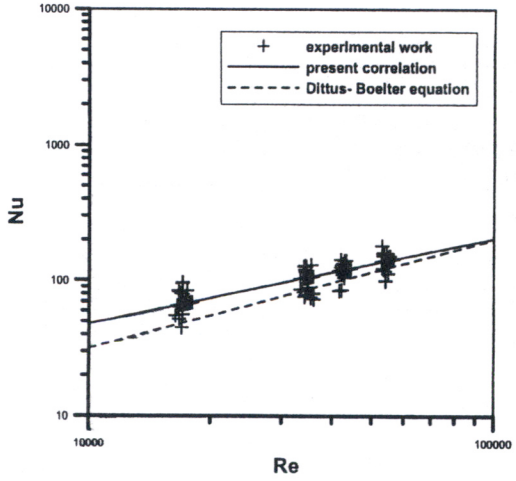

Fig.11 Comparison of the experimental data for Nu with the present correlation and with a published correlation of another author.